Published in final edited form as:
J Immunol. 2008 June 15; 180(12): 8211–8221.

The TCR's α-CPM promotes close approximation of the CD8 co-receptor allowing efficient signal initiation

Michel Mallaun[*], **Dieter Naeher**[*], **Mark A. Daniels**[*,†], **Pia P. Yachi**[‡], **Barbara Hausmann**[*], **Immanuel F. Luescher**[§], **Nicholas R.J. Gascoigne**[‡], and **Ed Palmer**[*]

[*]Laboratory of Transplantation Immunology and Nephrology, Department of Biomedicine, University Hospital Basel, Hebelstrasse 20, 4031 Basel, Switzerland [‡]Department of Immunology, The Scripps Research Institute, 10550 North Torrey Pines Road, La Jolla, California 92037, USA [§]Ludwig Institute for Cancer Research, Lausanne Branch, University of Lausanne, 1066 Epalinges, Switzerland

Abstract

The CD8 co-receptor contributes to the recognition of peptide-MHC (pMHC) ligands by stabilizing the TCR-pMHC interaction and enabling efficient signaling initiation. It is unclear though, which structural elements of the TCR ensure a productive association of the co-receptor. The α-chain connecting peptide motif (α-CPM) is a highly conserved sequence of eight amino acids in the membrane proximal region of the TCR α-chain. TCRs lacking the α-CPM respond poorly to low-affinity pMHC ligands and are unable to induce positive thymic selection. Here we show that CD8 participation in ligand binding is compromised in T lineage cells expressing mutant α-CPM TCRs, leading to a slight reduction in apparent affinity; however, this by itself does not explain the thymic selection defect. By fluorescence resonance energy transfer (FRET) microscopy, we found that TCR-CD8 association was compromised for TCRs lacking the α-CPM. While high-affinity (negative-selecting) pMHC ligands showed reduced TCR-CD8 interaction, low-affinity (positive-selecting) ligands completely failed to induce molecular approximation of the TCR and its' co-receptor. Therefore, the TCR's α-CPM is an important element in mediating CD8 approximation and signal initiation.

Keywords

T Cells; T Cell Receptors; Cell Activation; Signal Transduction; Thymus

Introduction

Upon binding a peptide-MHC ligand, the αβ T-cell receptor complex initiates an intracellular signal; when a T-cell or thymocyte accumulates a sufficient number of TCR and other signals, a cellular response is induced. An important element in TCR signal initiation is the co-receptor, either CD4 or CD8. These co-receptors bind to MHC class II or class I molecules, respectively (1–4). The co-receptor binding site on an MHC molecule is distinct from its' peptide-binding

Correspondence Address Ed Palmer Laboratory of Transplantation Immunology and Nephrology, Department of Biomedicine, University Hospital Basel, Hebelstrasse 20, 4031 Basel, Switzerland Phone: +41 61 265 31 20 Fax: +41 61 265 34 20 ed.palmer@unibas.ch.
[†]Present address: Department of Molecular Microbiology and Immunology, University of Missouri-Columbia, One Hospital Drive, Columbia, MO 65212, USA

Disclosures The authors declare that they have no conflict of interest with this manuscript.

domain and therefore doesn't interfere with TCR binding (5). By binding to the same MHC molecule as the TCR (6), the co-receptor increases the overall-affinity of TCR-pMHC binding (7,8). Moreover, the CD4 and CD8 co-receptors are important for signal initiation due to their association with the tyrosine kinase, Lck (9), which is required for critical early events in TCR signaling (10–12). Lck phosphorylates the ITAMs of the CD3 molecules within the TCR complex, especially those of CD3ζ (13). Moreover, Lck phosphorylates tyrosine residues on the syk family kinase, Zap-70 (14), thereby increasing Zap-70's enzymatic activity (15). These are. Therefore the co-receptor has an important function in coupling ligand binding with the initiation of signal transduction.

While high-affinity TCR-pMHC interactions exhibit some degree of CD8 independence, lower affinity interactions (K_D values $\geq 3\mu M$) require CD8 for antigen recognition (16). In the absence of CD8 binding to pMHC, primary CD8 T-cells fail to form conjugates with APCs, even in the presence of high concentrations of antigenic peptide (17). In this context, the CD8αβ heterodimer, but not the CD8αα homodimer significantly increases the avidity of TCR-mediated ligand recognition, as measured by binding to soluble monomeric pMHC (18). The same study suggests that CD8β facilitates TCR signal induction not only by increasing the avidity of TCR-ligand binding, but also by docking TCR/CD3 to glycolipid-enriched microdomains (GEMs).

During thymocyte development, the ability of the TCR to read ligand affinity plays an important role in establishing a self-tolerant T-cell repertoire (19,20). Pre-selection $CD4^+CD8^+$ double positive (DP) thymocytes expressing a MHC I restricted TCR, respond to self-antigens by differentiating into mature $CD8^+$ single positive (SP) thymocytes, if the apparent affinity of TCR-CD8 / pMHC binding is below a discrete threshold ($K_D > 6\ \mu M$) (21). On the other hand, pre-selection DP thymocytes, whose TCRs bind self pMHC antigen with an apparent affinity above the selection threshold ($K_D < 6\ \mu M$) initiate apoptosis and fail to develop into mature T lineage cells (21). In this way, overtly self-reactive T-cells are removed (negatively selected) from the developing T-cell repertoire. The co-receptors play an important role in the selection outcome (22,23). For example, CD8β deficient mice select severely reduced numbers of MHC I restricted cytotoxic T-cells (24,25).

Exactly how the co-receptor and TCR interact to initiate distinct signals with defined cellular consequences is not completely understood. The TCR α-chain contains an evolutionarily conserved motif in its constant region, termed the α-chain connecting peptide motif (α-CPM). Mutations in this conserved membrane proximal motif (FETDxNLN) promote unresponsiveness to antigenic stimuli (26) and defects in positive selection; interestingly, negative selection with an agonist ligand was unaffected (27,28). TCR/CD3 complexes where the α-CPM has been substituted with amino acids from the TCRδ membrane proximal domain exhibit a reduced association with the CD3δ subunit (27). Interestingly, thymocytes from CD3δ deficient mice are defective in undergoing positive selection as well, implying a role of CD3δ in linking TCR and co-receptor molecules (29). Finally, α-CPM deficient TCRs bind agonist ligands as well as wild type TCRs, but cannot cooperate with CD8 to increase ligand binding (30). This further supports the idea that the α-CPM may mediate a molecular interaction between CD8 and the TCR, either directly or via CD3δ.

In order to directly measure the role of the α-CPM in the TCR-CD8 interaction, we measured FRET between fluorescently tagged CD3ζ (of the TCR complex) and CD8β (31,32). We used a well-defined set of peptides, inducing positive or negative selection of thymocytes expressing the OT-I TCR (33) to assess the role of the α-CPM in mediating an interaction between CD3ζ and CD8β. In T-cell hybridomas expressing either a wildtype or α-CPM mutant OT-I TCR, CD3ζ-CD8β interactions within the immunological synapse (34) varied in both intensity and time. While negative selecting peptides induced fast and sustained FRET signals in

hybridomas expressing the wildtype OT-I TCR, positive selecting peptides induced markedly delayed and weaker FRET signals. T-cell hybridomas expressing α-CPM deficient TCRs exhibited diminished and delayed CD3ζ-CD8β interactions in response to negative selecting peptides. Strikingly, positive selecting peptides did not induce detectable CD3ζ-CD8β interactions, even though both TCR/CD3 complexes and CD8 molecules were efficiently recruited to the synapse. Since the α-CPM is located in the constant domain of every TCR and does not interfere with the TCR's specificity (30), we suggest a role for the α-CPM in translating low affinity TCR-pMHC binding across the plasma membrane by ensuring a close association of the co-receptor to the TCR.

Materials and Methods

Peptides and antibodies

OVA variant peptides were synthesized and purified as described (20) (35) and had the following affinity hierarchy for the OT-I TCR: OVA > Q4 > Q4R7 > T4 > Q4H7 > G4 > E1 >> VSV (33). Anti-CD8β (53–5.8), anti-H-2K^b (AF6-88.5), anti-TCRβ (H57-597), anti-Vα2 (B20.1), capturing anti-mIL-2 (JES6-1A12) and detecting anti-mIL-2-biotin (JES6-5H4) are from BD Biosciences. Rabbit monoclonal anti-GFP is form Epitomics, mouse monoclonal anti-GFP is from Santa Cruz Biotechnology, anti-phospotyrosine (4G10) is from Upstate.

DNA Constructs

The OT-I TCR comprises rearranged TCRα (Vα2-Jα26) and TCRβ (Vβ5-Dβ2-Jβ2.6) chains and is derived from the K^b-restricted, OVA$_{257–264}$-specific CTL clone, 149.42 (36). The cDNAs encoding the OT-Iα and OT-Iβ wildtype chains were recovered by standard PCR techniques from retroviral vectors described earlier (37) and ligated into the *Bam*HI and *Xho*I sites of the lentiviral expression vector pTRIPΔU3EF1αEGFP (N. Taylor, Montpellier), replacing the *Bam*HI-EGFP-*Xho*I fragment. Resulting plasmids were referred to as pTRIPΔU3EF1α-OTIα and pTRIPΔU3EF1α-OTIβ, respectively. cDNAs encoding the OT-I TCR αδ chimeras were constructed using the previously described II and IV chimeric cDNAs (26) encoding the 3BBM74 TCR (38). The *Spe*I-*Xho*I fragment of pTRIPΔU3EF1α-OTIα was replaced by the corresponding fragment from the αII or αIV chimeric α-chain. Similarly, the OT-Iβγ chimera III was constructed by replacing the *Xba*I-*Xho*I fragment of pTRIPΔU3EF1α-OTIβ with the corresponding chimeric βIII fragment (26). The CD8β-YFP (32) and CD3ζ-CFP (31) constructs have been described.

Fetal thymic organ culture

Fetal thymic organ culture (FTOC) was performed as described (19). In brief, thymic lobes were excised from OT-I Rag−/− β2m −/− transgenic mice at a gestational age of day 15.5. FTOCs included exogenous β2m (5μg/ml) and peptide (2μM for negative-selecting peptides and 20μM for positive selecting ligands). After 7 days of culture, thymocytes were subjected to flow cytometry analysis.

Ligand binding

Tetramer binding studies were performed as described (33). In brief, DP thymocytes from OT-I Rag−/− β2m−/− mice were stained with fluorescently labeled tetramers and K_D values were determined by nonlinear regression analysis of the mean fluorescence intensities. Differences related to the replacement of the α-CPM (ΔK_D) were calculated as ratios between the α-CPM and the OT-I wildtype K_D values. Monomer binding studies were performed as described (21). In brief, the ratio r of free TCR was determined by two-step photoaffinity labeling of DP thymocytes from T1 Rag−/− β2m−/− mice. Ligand concentration-dependent binding curves

were analyzed by nonlinear regression and K_D values were determined. ΔK_D values were calculated between the α-CPM and the TM control K_D values.

Cells

Supernatants of Phoenix packaging cells (G. Nolan, UK) were used to transduce the TCR/CD8-deficient hybridoma 58 (39) sequentially with constructs for CD8α CD8β-YFP and CD3ζ-CFP. Resulting hybridomas were sorted for high CFP and YFP expression. To introduce the wild-type or chimeric OT-I α chains and the wild-type or chimeric OT-I β chains, $CaCl_2$-based transfection of 293T cells was used to produce lentiviral supernatants for subsequent transduction.

Transduced hybridomas were FACS-sorted for similar TCR expression among wildtype, mutant α-CPM and TM control hybridomas. All cells were grown in RPMI supplemented with 4% FCS, 2 mM L-glutamine, 100 U/ml penicillin, 100 μg/ml streptomycin, and 50 μM β-mercaptoethanol.

Microscopy

An Olympus IX81 inverted microscope was used in this study. A triggered F-ViewII camera was attached to the microscope and the MT20 illuminator with a 150W Xenon lamp (Olympus). The system was run by CellR software (Olympus). Optical filter cubes on an automated turret were used to change excitation and emission corresponding to the various channels. The filter cubes had the following spectral alignments (center/bandpass): YFP excitation, 500/20 nm; YFP emission, 535/30 nm; CFP excitation, 436/20 nm; CFP emission, 480/40 nm. The FRET filter cube was a combination of the CFP excitation filter and the YFP emission filter. Beamsplitting was achieved with a 455 nm long pass dichroic mirror in the CFP filter cube and with a 515 nm long pass dichroic mirror in the YFP and FRET filter cubes. A 60x, 1.4– numerical aperture oil objective was used.

FRET and recruitment analysis

For CFP and YFP, the efficiency of energy transfer is greater than 50% within the Förster Radius R_0 of 4.9 – 5.2 nm and approximates zero beyond 2x R_0 (~10nm). Crosstalk coefficients of CFP fluorescence into the FRET channel (=d) and YFP into the FRET channel (=a) were calibrated using hybridomas transduced with either CD3ζ-CFP or CD8β-YFP alone. For the specified filter cubes they were d=36.8% and a=18.1%. For each image, the CFP, YFP and FRET channel was acquired using the 3 specified filter cubes. Background was subtracted as averaged signal from a user-specified, cell-free region of each image. To calculate the FRET efficiency the following formula was used: $E = (FRET - a \cdot CFP - d \cdot YFP)/(FRET - a \cdot CFP - d \cdot YFP + G \cdot CFP)$, which was described earlier (31) (40). G is the independently calibrated ratio of sensitized emission in the FRET channel before photobleaching to donor recovery in the CFP channel after acceptor photobleaching (41). For the imaging system used here, $G = 1.7 \pm 0.1$. FRET efficiencies were calculated from hybridoma:APC interfaces. For illustration, the ImageJ software was used and calculated FRET efficiency images were illustrated in pseudo-colors. Statistical analysis of E was performed using Student's two-sample t-test assuming two-tailed distribution and unequal variance. The recruitment of fluorescently tagged proteins to the synapse was calculated as background-corrected ratio of the MFI of the synapse region divided by the MFI of a user-defined membrane region, outside of the synapse.

APC peptide loading

Tap2 deficient RMA-S cells (42) were loaded with exogenous OVA peptide variants described above. We varied the loading concentration of each peptide to generate similar pK^b expression. RMA-S cells were incubated at 29 °C overnight followed by peptide addition for 30min at 29

°C and incubation for 3h at 37 °C. pMHC surface expression was assessed by anti-H-2K^b-PE staining and flow cytometry analysis.

IL-2 release assay

For IL-2 detection, 96-well flat-bottomed ELISA plates (Nunc MaxiSorp) were coated with 60μl anti-IL-2 at 2 ug/ml in PBS 0.02% NaN_3 overnight at 4 °C. For antigen stimulation, 10^5 OT-I hybridomas and 10^5 peptide-pulsed RMA-S cells were incubated in flat-bottomed wells for 24h at 37 °C. 100μl of the supernatant was added to the washed and blocked ELISA plates for 1h at room temperature. Anti-mIL-2-biotin secondary antibody was applied at 2 μg/ml for 1h at room temperature. Streptavidin-HRP (Zymed) was applied at 0.3 ug/ml for 1h at room temperature. Conversion of 0-Phenylenediamine dihydrochloride (Sigma) was allowed for 5min in the dark followed by stopping the reaction with 50μl 10% H_2SO_4 per well. OD_{490nm} was detected and normalized to a standard dilution series by the Softmax Pro software Molecular Devices).

TCR downregulation

10^5 OT-I hybridomas and 10^5 peptide-pulsed RMA-S cells were incubated in flat-bottomed wells at 37 °C. Cells were fixed with 2% formaldehyde, washed and stained for Vβ5 and analyzed by flow cytometry. Data were presented as the percentage of TCRs remaining on the cell surface.

Stimulation of hybridomas for FRET analysis

2×10^5 OT-I hybridomas and 2×10^5 peptide-pulsed RMA-S cells were incubated in flat-bottomed wells at 37 °C. Stimulation was stopped by fixation with 2% formaldehyde. Cells were washed with PBS, 10 mM Tris and finally with buffer C of the Slowfade antifade kit (Invitrogen). Cells were mounted on standard glass slides in Slowfade antifade mounting medium.

Immunoprecipitation and immunoblots

2×10^7 hybridomas and 2×10^7 peptide-pulsed RMA-S cells were incubated in round-bottomed tubes at 37 °C. Cells were lysed in 1% Triton X-100, 50 mM Tris pH 7.5, 150 mM NaCl, 1 mM EDTA, 20 mM β-glycerophosphate, 1 mM Na_3VO_4, 10 mM NaF, 1 mM PMSF, 2 μg/ml aprotinin, 5 μg/ml leupeptin and 1 mg/ml pefabloc. Lysates were precleared by centrifugation and with Protein G Sepharose beads and were immunoprecipitated overnight with rabbit monoclonal anti-GFP (Epitomics). After washing, samples were separated by 10% reducing SDS-PAGE, blotted and probed with anti-phosphotyrosine (4G10; Upstate) followed by anti-mouse-HRP (Cell Signaling) and ECL detection (GE Healthcare). For a loading control, membranes were stripped and probed with mouse monoclonal anti-GFP (Santa Cruz).

Results

Wildtype and α-CPM mutant TCRs

The wildtype and chimeric TCRs used in this study are schematically represented in Fig. 1A. As point mutations in the α-CPM led to abrogation of surface TCR expression (26), we generated chimeric TCRs that contain corresponding domains from the γδ TCR which lacks the α-CPM. Fig. 1A shows the membrane proximal connecting peptide (CP), transmembrane (TM) and cytoplasmic (Cyto) domains of the constant regions of the receptors used in this study. The α-CPM is indicated with an asterisk (*), TCR δ sequences that replace α-sequences are shown in light grey and TCR γ sequences that replace β-sequences are shown in dark grey. The α-CPM mutant chain (αIV) is a chimera encoding V, J and parts of the C domain from the TCR α-chain followed by a segment of Cδ, which lacks the α-CPM. The βIII chain encodes

V, D, J and part of the C domain from the TCR β-chain followed by Cγ transmembrane and cytoplasmic regions. The trans-membrane control receptor (TM) is composed of the βIII chain and the αII chain, which is identical to the αIV chain except that it contains the α-CPM (Fig. 1A).

Therefore, the TM control receptor and the α-CPM mutant receptor are distinguished by the presence or absence of the α-CPM. The variable regions and the bulk of the constant regions among the various receptors were identical and were not affected by the replacements of the domains shown in Fig. 1A.

Defective positive selection in α-CPM mutant mice

Thymocytes from Rag−/− mice expressing transgenic wildtype or α-CPM mutant TCRs were analyzed to determine the influence of the α-CPM on thymic selection. As previously shown, wildtype OT-I transgenic thymocytes generated substantial numbers of CD8αβ+ CD4− single positive (SP) cells (19,43), whereas only very limited numbers of α-CPM mutant thymocytes were positively selected (Fig. 1B) (28). Similarly, in the T1 TCR transgenic system (21), CD8αβ SP cells were generated in the wildtype and TM control transgenic mice but not in α-CPM mutant mice, clearly indicating a positive selection defect (Fig. 1C).

The ability of different OVA variant peptides to induce positive or negative selection (see materials and methods for affinity hierarchy) was tested in fetal thymic organ culture (FTOC) (19). As shown here (Fig. 1D) and previously (33), the strong OVA, Q4 and Q4R7 ligands induced negative selection in FTOC, as indicated by a low percentage of CD8αβ+ CD4− SP thymocytes. On the other hand, the weak ligands Q4H7 and E1 generated substantial numbers of CD8αβ+ CD4− SP cells, which is indicative of positive selection (Fig. 1D and (33)). The non-cognate VSV ligand induced neither positive nor negative selection, reflected by high numbers of CD8αβ+ CD4+ double positive (DP) thymocytes. In contrast to wildtype OT-I thymocytes, α-CPM mutant thymocytes exhibited a substantially different selection outcome in response to the various peptides (Fig. 1E). Only OVA was identified as negative selector, given the paucity of CD8αβ + CD4− SP cells. All other ligands were non-selectors of α-CPM mutant thymocytes; the presence of high numbers of DP thymocytes and relatively few SP thymocytes indicate the lack of positive or negative selection (Fig. 1E).

Ligand Binding

The lack of selection in α-CPM mutant FTOCs might indicate that the α-CPM mutant receptor cannot bind cognate ligands. To determine the influence of the α-CPM mutation on ligand binding, we performed pMHC tetramer and monomer binding studies. Both binding assays involved concomitant TCR and CD8 co-receptor binding to the MHC and were performed on pre-selection DP thymocytes at 37°C. α-CPM mutant thymocytes exhibited decreased ligand binding compared to OT-I wildtype thymocytes, when incubated with fluorescently labeled pMHC tetramers (Fig. 2A). Dissociation constants (K_D) were calculated by nonlinear regression analysis of the mean fluorescence intensities of bound tetramers. Relative to wildtype OT-I thymocytes, α-CPM mutant thymocytes bound all tetramers tested less avidly. The reduction of tetramer avidity (ΔK_D) was 3 to 4 fold (Table 1A).

Binding studies using monomeric pMHC ligands (44) (21) involve peptide ligands that carry a photoreactive group that can be photochemically crosslinked to the TCR upon specific ligand binding. Concentration dependent binding curves were analyzed by nonlinear regression and K_D values were calculated. For low affinity (positive selecting) ligands, half-maximal TCR saturation was not reached (data not shown) and therefore K_D values could not be determined. Similar to the tetramer binding experiments, DP thymocytes from α-CPM mutant T1 mice bound pMHC ligands with ~4 fold lower apparent affinity (Table 1B) compared to wildtype

or TM control thymocytes. The reduced apparent affinity of α-CPM mutant DP thymocytes to bind pMHC could be attributed to defective cooperativity between TCR and CD8, as ligand binding was similar when the interaction between CD8 and MHC was disrupted by point mutations in the MHC (Fig. 2B, 4P-K^d Δ223/227) (21). In both the tetramer and monomer binding experiments, the 3–4 fold decrease in ligand binding displayed by α-CPM mutant thymocytes was similar for all ligands (Table I) and was independent of TCR specificity (i.e. similar affinity decreases were observed for OT-I TCR and T1 TCR expressing thymocytes). Since the CD8 co-receptor is also involved in TCR signaling initiation, we wondered whether the α-CPM mutation might affect signal initiation as well. To test this hypothesis, we set up a system to observe TCR-CD8 interaction directly by FRET microscopy.

Expression of wildtype and mutant OT-I TCRs and functional expression of chimeric fluorescent constructs in hybridomas

The TCR/CD8-deficient hybridoma 58 was successively transfected with constructs for CD8α, CD8β-YFP, CD3ζ-CFP and TCR chains for the wildtype, mutant α-CPM or TM control receptors. Resulting OT-I wildtype, α-CPM mutant and TM control T-cell hybridomas were FACS sorted for similar expression of TCR-Vα2, CD8α (data not shown), CD8β-YFP and CD3ζ-CFP (Fig. 3A). CD3ζ-CFP surface expression was assessed by fluorescence microscopy of T-cell hybridomas before and after transduction or the OT-I wt TCR (Fig. 3B). Plasma membrane expression of CD3ζ-CFP was only observed in TCR-positive cells. The localization of CD3ζ-CFP at the plasma membrane was observed for the wildtype and both chimeric receptors (data not shown) indicating that CD3ζ-CFP was assembled in surface TCR/CD3 complexes. Moreover, the CD3ζ-CFP molecules were tyrosine phosphorylated upon pervanadate treatment, pointing to its functionality in wildtype, TM control and mutant hybridomas (Fig. 3C).

Antigen-dependent stimulation of wildtype and α-CPM mutant OT-I T-cell hybridomas

For antigen presenting cells, we used RMA-S murine lymphoma cells expressing H-$2K^b$ loaded with exogenously added individual peptides (42). RMA-S-H-$2K^b$ cells were pulsed with indicated peptides at concentrations yielding similar surface expression of pK^b (Fig. 4A). To assess functional responses, we tested hybridomas for their ability to internalize the TCR and to release IL-2 upon stimulation with peptide loaded APCs. The high-affinity/negative-selecting ligands OVA and Q4R7 induced ~35% TCR endocytosis in OT-I wildtype or TM control hybridomas after 60min of incubation (Fig. 4B). The positive-selecting ligand Q4H7 showed slightly decreased and delayed kinetics of TCR endocytosis. In contrast, the lower affinity positive-selecting ligand G4 failed to induce detectable loss of TCR from the cell surface, similar to the non-cognate ligand VSV. In the α-CPM mutant hybridomas, TCR endocytosis was substantially reduced, implicating a role for the α-CPM in the early cellular response to antigen. As readout for a late cellular response, we examined IL-2 release. The negative selecting ligands OVA and Q4R7 induced IL-2 secretion from wildtype and TM control hybridomas (Fig.4C). Neither the positive-selecting Q4H7 ligand nor the non-cognate VSV ligand produced detectable amounts of IL-2 (Fig. 4C). The α-CPM mutant hybridomas failed to produce IL-2 in response to any of the ligands, excluding the possibility that the α-CPM mutant cells could accumulate weak signals over time, which would not be detected by measuring TCR internalization.

Antigen-induced CD3ζ-CD8 interaction

The approximation of two molecules within 10 nm is an indirect measure of their interaction and can be assessed by FRET imaging (40). For CFP and YFP, the efficiency of energy transfer is greater than 50% within a radius of ~5 nm and approximates zero beyond ~10 nm. Since the αβ TCR has a diameter of ~10 nm (7), significant FRET between CFP and YFP strongly

suggests physical interaction between the carrier molecules CD3ζ and CD8β used in these studies. We compared the FRET signals induced between CD3ζ-CFP and CD8β-YFP in the T-cell hybridomas upon stimulation with peptide loaded APCs. Following stimulation of OT-I wildtype hybridomas with OVA-loaded RMA-S cells, CD3ζ-CFP and CD8β-YFP were recruited to the synapse, where the FRET efficiency increased significantly (Fig. 5A upper panel). Stimulation with the non-cognate VSV ligand did not recruit CD3ζ-CFP to the synapse andconsequently no significant FRET was detected (Fig. 5A lower panel). CD8β-YFP was recruited to the APC contact area even with the non-cognate VSV ligand, as previously observed (32). In contrast, α-CPM mutant hybridomas efficiently recruited both CD3ζ-CFP and CD8β-YFP to the synapse but failed to induce substantial FRET (Fig. 5A middle panel). In time-course experiments (Fig. 5B), the high-affinity, negative-selecting ligands OVA and Q4R7 induced a fast and sustained FRET between CD3ζ-CFP and CD8β-YFP in OT-I wildtype and TM control hybridomas, whereas the low-affinity, positive-selecting ligands Q4H7 and G4 induced a delayed and weaker FRET signal. It is noteworthy that with the positive-selecting Q4H7 ligand, whose affinity for the OT-I receptor is only 2–3x lower than the negative selector Q4R7 (33), the FRET signal developed significantly more slowly. However, by 60min the FRET signal induced by Q4H7 reached a similar intensity as that induced by negative-selecting ligands (Fig. 5B). In the mutant α-CPM hybridomas FRET signals were markedly reduced, pointing towards a defect in CD3ζ-CD8β approximation (Fig. 5B middle panel). Strikingly, in absence of the α-CPM the low-affinity ligands Q4H7 and G4 caused no detectable CD3ζ-CD8β interaction over background (Fig. 5B). The reduced FRET signals in the α-CPM mutant hybridomas could not be attributed to reduced TCR or CD8 recruitment to the synapse since CD3ζ-CFP and CD8β-YFP are recruited similarly as in OT-I wildtype or TM control hybridomas (Fig. 5C and 5D). Therefore, an intact α-CPM is required for cytoplasmic approximation of the CD8 co-receptor and the TCR for low-affinity ligands, explaining the defect in positive selection in α-CPM deficient mice.

Antigen induced TCR-CD8 interaction correlates with CD3ζ phosphorylation

To test whether TCR-CD8 association at the plasma membrane correlates with the initiation of intracellular signaling, we directly examined the phosphorylation of CD3ζ-CFP, an early event in TCR signal transduction (24) (45). For this Western blot analysis, the same time points were chosen as in the microscopy-based FRET experiments. The OT-I wt and TM control hybridomas exhibited similar patterns of CD3ζ-CFP phosphorylation (Fig. 6A and 6C). The high-affinity/negative-selecting ligands OVA and Q4R7 induced rapid and sustained phosphorylation of CD3ζ-CFP, whereas the low-affinity/positive selecting ligand Q4H7 triggered delayed and weaker phosphorylation of CD3ζ-CFP. In the α-CPM mutant hybridomas only moderate phosphorylation was observed at late time points in response to the high-affinity ligands OVA and Q4R7 while almost no phosphorylation was induced by the positive selecting ligand Q4H7 (Fig. 6B). The non-cognate VSV ligand failed to induce phosphorylation in any of the hybridomas. Therefore, the extent and kinetics of TCR-CD8 interaction as measured by FRET correlates with the extent and kinetics of CD3ζ-CFP phosphorylation (Fig. 5B and Fig 6D).

Discussion

TCRs lacking the α-CPM are recruited to the synapse but do not efficiently interact with the CD8 co-receptor. Our FRET experiments indicate that close approximation of the two molecules is delayed and reduced when α-CPM mutant T-cell hybridomas encounter a strong ligand and completely absent if they encounter a weak ligand. Therefore, the defective transmission of weak signals in the α-CPM mutant TCR (28) is a consequence of deficient TCR-CD8 interaction and subsequent decreased CD3ζ phosphorylation. We previously showed that thymocytes expressing an α-CPM mutant TCR fail to be positively selected,

independent of the TCR specificities tested (27,28). Here, we showed that positive selectors and weak negative selectors fail to induce any form of thymic selection; only the strong agonist, OVA induces negative selection in α-CPM mutant FTOCs. Previous studies performed with hybridoma cells showed a defect of TCR-CD8 cooperation in binding to pMHC (30). To quantify this binding defect we measured TCR ligand binding on thymocytes of OT-I and T1 TCR transgenic mice expressing wildtype or mutant α-CPM constant regions. A ~4 fold reduction in TCR binding affinity (Fig. 2 and Table I) could be measured between wildtype and α-CPM mutant TCRs; this difference in ligand binding was not evident with pMHC ligands that fail to engage CD8 (Fig. 2B and Table IB, 4P-K^d Δ223/227). Therefore, reduced pMHC binding of α-CPM mutant TCRs could be attributed to defective TCR-CD8 cooperation and not to altered TCR affinity *per se*. Moreover, this demonstrates that putative structural alterations in the α-CPM mutant TCR do not affect TCR affinity. Nevertheless, the slight reduction in apparent affinity of α-CPM deficient TCRs did not fully explain their thymic selection defects (Fig. 1).

To more fully understand the mechanism, by which α-CPM mutant receptors fail during thymic selection, we used a T-cell hybridoma, expressing labeled CD8β and CD3ζ molecules (32). Our experiments confirm previous work (32) that the CD8 co-receptor is recruited to the synapse similarly for all pMHC ligands (Fig. 5D), whereas the extent of TCR/CD3 recruitment correlated with ligand affinity (Fig 5C and (46)). Measuring FRET between CD8β-YFP and CD3ζ-CFP in the synapse, which reflects CD8β-CD3ζ interaction, we observed different interaction kinetics for negative- and positive selecting ligands. Negative selecting ligands induce a rapid and sustained FRET signal, whereas positive selecting ligands induce slow and delayed FRET (Fig. 5B), extending a previous study (46). Here, we show that the transition between the FRET patterns induced by negative or positive selecting ligands (Fig. 5A) correlates with the affinity selection threshold previously described (33). These data demonstrate that positive selecting pMHC ligands exhibit reduced TCR-CD8 interaction in the synapse compared to negative selecting ligands, which correlates with decreased CD3ζ phosphorylation during signal initiation in response to positive selecting ligands (Fig 6A, (33)).

Our data further show that the absence of the α-CPM has no discernible effect on TCR or CD8 recruitment to the IS (Fig 5C,D). Both CD8 and TCR/CD3 were similarly recruited to the synapse in all cell lines studied (OT-I wt, α-CPM mutant and TM control (Fig. 5C and 5D)). Strikingly, CD8ζ-CD3ζ interaction was significantly reduced in T-cell hybridomas expressing α-CPM mutant receptors (Fig 5B). This emphasizes that TCR and co-receptor can be colocalized without any interaction as detected by FRET (31) (32). This reduction of molecular interaction under the plasma membrane had a clear functional consequence. Phosphorylation of CD3ζ was markedly reduced in α-CPM mutant hybridomas (Fig 6D). These data suggest that an important role of the α-CPM is to facilitate the physical approximation of the intracellular domain of CD8 to the TCR/CD3 complex, a requirement for ITAM phosphorylation.

FRET signals observed in α-CPM mutant hybridomas were not always predictive of selection outcome. The high affinity ligands OVA and Q4R7 induced similarly weak FRET signals in α-CPM mutant cells, similar to those observed in wildtype or TM control cells stimulated by positive-selecting ligands (Fig. 5B). In α-CPM mutant FTOCs, OVA is a negative selector, which might be expected since OVA can induce negative selection in wildtype OT-I FTOCs even in the absence of CD8 expression (47). Thus, negative selection in OVA stimulated α-CPM mutant FTOCs might occur even without the induction of FRET. On the other hand, Q4R7 is a non-selector in α-CPM mutant FTOCs (Fig. 1E), even though this ligand induces a similar FRET signal like OVA. It's possible that the fluorescent protein labels exaggerate the TCR-CD8 interaction induced by Q4R7, although we consider this less likely as mutant forms

of CFP and YFP were used that minimize spurious dimerization (32). Nevertheless, these data clearly show that the α-CPM mutation leads to a reduction in TCR-CD8 interaction; the corresponding FTOCs show the consequences of this weakened interaction on thymic selection.

We propose a model, where the lateral approximation of CD8 and the TCR is similar to the approximation of two sides of a zipper (Fig 7). The molecules are first brought together by the pMHC ligand and while the ligand remains bound to the receptor/co-receptor pair, their close apposition continues downward in the direction of the T-cell. The α-CPM functions as a zipper tooth on the TCR side of the CD8/TCR complex stabilizing the two sides of the zipper. If the membrane proximal domains of CD8 and TCR become “zipped”, the CD8 associated Lck can tyrosine phosphorylate the ITAMs of the TCR/CD3 complex. Once the positive selecting ligand dissociates, CD8 and the TCR disengage and Lck mediated phosphorylation is terminated. TCRs lacking the α-CPM might not stabilize the TCR-CD8 zipper, compromising ITAM phosphorylation.

Signaling by low affinity ligands, which occupy the TCR for a relatively short time, is severely affected by the lack of the α-CPM. Agonist ligands such as OVA could occupy the α-CPM mutant TCR for a sufficiently long time to compensate for the lack of an important tooth in the receptor/co-receptor zipper. Therefore, only the highest affinity ligands are capable of mediating negative selection in mutant α-CPM thymocytes (Fig 1). The α-CPM is present in the TCR α-chain throughout vertebrate evolution (26). α-CPM deficient receptors associate poorly with CD3δ and related work has previously shown that the CD3δ molecule is also required to establish a link between the TCR and the CD8 co-receptor (29). Therefore, the α-CPM and CD3δ seem to be required for an optimal functional interaction with the CD8 co-receptor and for recognition of low affinity ligands that mediate positive selection and homeostatic expansion of peripheral T-cells. The α-CPM may serve an equivalent function for the CD4 co-receptor, since a class II MHC restricted α-CPM mutant TCR also fails to generate positive selection signals (27).

Acknowledgments

The authors thank Dr. Naomi Taylor (CNRS UMR 5535, Montpellier, France) for viral vectors and packaging cell lines and E. Wagner for animal care. The animal experiments were carried out in accordance with the Federal and Cantonal laws of Switzerland.

Source of Support This work was supported by grants from the Swiss National Science Foundation, EURAPS, Novartis and Hoffmann La Roche to EP; NIH grant R01AI074074 to NRJG; US Cancer Research Institute to MAD; and T32HL07195-30 to PPY.

Abbreviations used in this paper

α-CPM, α-chain connecting peptide motif
CFP, Cyan Fluorescent Protein
DP, $CD4^+CD8^+$ double positive
FRET, Fluorescence Resonance Energy Transfer
FTOC, Fetal Thymic Organ Culture
GEM, Glycolipid-Enriched Microdomains
MFI, Mean Fluorescence Intensity
pMHC, peptide-MHC
SP, $CD4^-CD8^+$ single positive
TM control, Trans-Membrane control
YFP, Yellow Fluorescent Protein

References

1. Cammarota G, Schierle A, Takacs B, Doran D, Knorr R, Bannworth W, Guardiola J, Sinigaglia F. Identification of a CD4 binding site on the b2 domain of HLA-DR molecules. Nature 1992;356:799–781. [PubMed: 1574119]
2. Koenig R, Huang LY, Germain RN. MHC class II interaction with CD4 mediated by a region analogous to the MHC class I binding site for CD8. Nature 1992;356:796–798. [PubMed: 1574118]
3. Norment AM, Salter RD, Parham P, Engelhard VH, Littman VH. Cell-cell adhesion mediated by CD8 and MHC class I molecules. Nature 1988;336:79–81. [PubMed: 3263576]
4. Salter RD, Benjamin H, Wesley PK, Buxton SE, Garrett TPJ, Clayberger C, Krensky AM, Norment AM, Littman DR, Parham P. A binding site for the T-cell co-receptor CD8 on the alpha3 domain of HLA-A2. Nature 1990;345:41–46. [PubMed: 2109837]
5. Huang J, Edwards LJ, Evavold BD, Cheng Z. Kinetics of MHC-CD8 Interaction at the T Cell Membrane. J. Immunol 2007;179:7653–7662. [PubMed: 18025211]
6. Gallagher PF, de St Groth F, Miller JFAP. CD4 and CD8 molecules can physically associate with the same T-cell receptor. PNAS 1989;86:10044–10048. [PubMed: 2513572]
7. Garcia KC, Degano M, Stanfield RL, Brunmark A, Jackson MR, Peterson PA, Teyton L, Wilson IA. An alpha-beta T Cell Receptor Structure at 2.5 A and its Orientation in the TCR-MHC Complex. Science 1996;274:209–219. [PubMed: 8824178]
8. Wooldridge L, van den Berg HA, Glick M, Gostick E, Laugel B, Hutchinson SL, Milicic A, Brenchley JM, Douek DC, Price DA, Sewell AK. Interaction between the CD8 coreceptor and MHC class I stabilizes TCR-antigen complexes at the cell surface. J. Biol. Chem 2005;280:27491–27502. [PubMed: 15837791]
9. Veillette A, Bookman MA, Horak EM, Bolen JB. The CD4 and CD8 T cell surface antigens are associated with the internal membrane tyrosine-protein kinase p56lck. Cell 1988;55:301–308. [PubMed: 3262426]
10. Zamoyska R. CD4 and CD8: modulators of T-cell receptor recognition of antigen and of immune responses? Curr. Opin. Immunol 1998;10:82–87. [PubMed: 9523116]
11. Trobridge PA, Forbush KA, Levin SD. Positive and Negative Selection of Thymocytes Depends on Lck Interaction with the CD4 and CD8 Coreceptors. J. Immunol 2001;166:809–818. [PubMed: 11145654]
12. Molina TJ, Kishihara K, Siderovskid DP, van Ewijk W, Narendran A, Timms E, Wakeham A, Paige CJ, Hartmann KU, Veillette A, Davidson D, Mak TW. Profound block in thymocyte development in mice lacking p56lck. Nature 1992;357:161–165. [PubMed: 1579166]
13. Lewis LA, Chung CD, Chen J, Parnes JR, Moran M, Patel VP, Miceli MC. The Lck SH2 Phosphoryrosine Binding Site is Critical for Efficient TCR-Induced Processive Tyrosine Phosphorylation of the Zeta-Chain and IL-2 Production. J. Immunol 1997;159:2292–2300. [PubMed: 9278318]
14. van Oers NSC, Killeen N, Weiss A. Lck Regulates the Tyrosine Phosphorylation of the T Cell Receptor Subunits and ZAP-70 in Murine Thymocytes. J. Exp. Med 1996;183:1053–1062. [PubMed: 8642247]
15. LoGrasso PV, Hawkins J, Frank LJ, Wisniewski D, Marcy A. Mechanism of activation for Zap-70 catalytic activity. PNAS 1996;93:12165–12170. [PubMed: 8901551]
16. Holler PD, Kranz DM. Quantitative Analysis of the Contribution of TCR/pepMHC Affinity and CD8 to T Cell Activation. Immunity 2003;18:155–164. [PubMed: 12530984]
17. Potter TA, Grebe K, Freiberg B, Kupfer A. Formation of supramolecular activation clusters on fresh ex vivo CD8+ T cells after engagement of the T cell antigen receptor and CD8 by antigen-presenting cells. PNAS 2001;98:12624–12629. [PubMed: 11606747]
18. Arcaro A, Gregoire C, Bakker TR, Baldi L, Jordan M, Goffin L, Boucheron N, Wurm F, van der Merwe PA, Malissen B, Luescher IF. CD8beta Endows CD8 with Efficient Coreceptor Function by Coupling T Cell Receptor/CD3 to Raft-associated CD8/p56Lck Complexes. J. Exp. Med 2001;194:1485–1495. [PubMed: 11714755]
19. Hogquist KA, Jameson SC, Heath WR, Howard JL, Bevan MJ, Carbone FR. T cell receptor antagonist peptides induce positive selection. Cell 1994;76:17–28. [PubMed: 8287475]

20. Alam SM, Travers PJ, Wung JL, Nasholds W, Redpath S, Jameson SC, Gascoigne NRJ. T-cell-receptor affinity and thymocyte positive selection. Nature 1996;381:616–620. [PubMed: 8637599]
21. Naeher D, Daniels MA, Hausmann B, Guillaume P, Luescher I, Palmer E. A constant affinity threshold for T cell tolerance. J. Exp. Med 2007;204:2553–2559. [PubMed: 17938233]
22. Fung-Leung WP, Schilham MW, Rahemtulla A, Kündig TM, Vollenweider M, Potter J, van Ewijk W, Mak TW. CD8 is needed for development of cytotoxic T but not helper T cells. Cell 1991;65:443–450. [PubMed: 1673361]
23. Rahemtulla A, Fung-Leung WP, Schilham MW, Kündig TM, Sambhara SR, Narendran A, Arabian A, Wakeham A, Paige CJ, Zinkernagel RM, Miller RG, Mak TW. Normal development and function of CD8+ cells but markedly decreased helper cell activity in mice lacking CD4. Nature 1991;353:181–184.
24. Nakayama T, Singer A, Hsi ED, Samelson LE. Intrathymic signalling in immature CD4+CD8+ thymocytes results in tyrosine phosphorylation of the T-cell receptor zeta chain. Nature 1989;341:651–655. [PubMed: 2477711]
25. Fung-Leung WP, Kündig TM, Ngo K, Panakos J, De Sousa-Hitzler J, Wang E, Ohashi PS, Mak TW, Lau CY. Reduced Thymic Maturation but Normal Effector Function of CD8+ T Cells in CD8beta Gene-targeted Mice. J. Exp. Med 1994;180:959967.
26. Baeckstroem BT, Milia E, Peter A, Jaureguiberry B, Barldari CT, Palmer E. A motif within the T cell receptor a chain constant region connecting peptide domain controls antigen responsiveness. Immunity 1996;5:437–447. [PubMed: 8934571]
27. Baeckstroem BT, Mueller U, Hausmann B, Palmer E. Positive selection through a motif in the ab T cell receptor. Science 1998;281:835–838. [PubMed: 9694657]
28. Werlen G, Hausmann B, Palmer E. A motif in the ab T-cell receptor controls positive selection by modulating ERK activity. Nature 2000;406:422–426. [PubMed: 10935640]
29. Doucey MA, Goffin L, Naeher D, Michielin O, Baumgärtner P, Guillaume P, Palmer E, Luescher IF. CD3delta Establishes a Functional Link between the T Cell Receptor and CD8. J. Biol. Chem 2003;278:3257–3263. [PubMed: 12215456]
30. Naeher D, Luescher IF, Palmer E. A role for the a-chain connecting peptide motif in mediating TCR-CD8 cooperation. J. Immunol 2002;169:2964–2972. [PubMed: 12218110]
31. Zal T, Zal A, Gascoigne NRJ. Inhibition of T cell receptor-coreceptor interactions by antagonist ligands visualized by live FRET imaging of the T-hybridoma immunological synapse. Immunity 2002;16:521–535. [PubMed: 11970876]
32. Yachi PP, Ampudia J, Gascoigne NRJ, Zal T. Nonstimulatory peptides contribute to antigen-induced CD8-T cell receptor interaction at the immunological synapse. Nature Immunology 2005;6:785–792. [PubMed: 15980863]
33. Daniels MA, Teixeiro E, Gill J, Hausmann B, Roubaty D, Holmberg K, Werlen G, Hollaender GA, Gascoigne NRJ, Palmer E. Thymic selection threshold defined by compartmentalization of Ras/MAPK signalling. Nature 2006;444:724–729. [PubMed: 17086201]
34. Grakoui A, Bromley SK, Sumen C, Davis MM, Shaw AS, Allen PM, Dustin ML. The Immunological Synapse: A Molecular Machine Controlling T Cell Activation. Science 1999;285:221–227. [PubMed: 10398592]
35. Santori FR, Kieper WC, Brown SM, Lu Y, Neubert TA, Johnson KL, Naylor S, Vukmanovic S, Hogquist KA, Jameson SC. Rare, Structurally Homologous Self-Peptides Promote Thymocyte Positive Selection. Immunity 2002;17:131–140. [PubMed: 12196285]
36. Kelly JM, Sterry SJ, Cose S, Turner SJ, Fecondo J, Rodda S, Fink PJ, Carbone FR. Identification of conserved T cell receptor CDR3 residues contacting known exposed peptide side chains from a major histocompatibility complex class I-bound determinant. Eur. J. Immunol 1993;23:3318–3326. [PubMed: 8258346]
37. Stotz SH, Bollinger L, Carbone FR, Palmer E. T cell receptor (TCR) antagonism without a negative signal: evidence from t cell hybridomas expressing two independent TCRs. J. Exp. Med 1999;189:253–263. [PubMed: 9892608]
38. DiGiusto DL, Palmer E. An analysis of sequence variation in the beta chain framework and complementarity determining regions of an alloreactive T cell receptor. Mol. Immunol 1994;31:693–670. [PubMed: 7518035]

39. Letourneur F, Malissen B. Derivation of a T cell hybridoma variant deprived of functional T cell receptor alpha beta chain transcripts reveals a nonfunctional alpha-mRNA of BW5147 origin. Eur. J. Immunol 1989;19:2269–2274. [PubMed: 2558022]
40. Zal T, Gascoigne NRJ. Using live FRET imaging to reveal early protein-protein interactions during T cell activation. Curr. Opin. Immunol 2004;18:418–427. [PubMed: 15245734]
41. Zal T, Gascoigne NRJ. Photobleaching-Corrected FRET Efficiency Imaging of Live Cells. Biophys. J 2004;86:3923–3939. [PubMed: 15189889]
42. Ljunggren HG, Stam NJ, Oehlen C, Neefjes JJ, Hoeglund P, Heemels MT, Bastin J, Schumacher TNM, Townsend A, Kaerre K, Ploegh HL. Empty MHC class I molecules come out in the cold. Nature 1990;346:476–481. [PubMed: 2198471]
43. Clarke SR, Barnden M, Kurts C, Carbone FR, Miller JF, Heath WR. Characterization of the ovalbumin-specific TCR transgenic line OT-I: MHC elements for positive and negative selection. Immunology & Cell Biology 2000;78:110–117. [PubMed: 10762410]
44. Luescher IF, Cerottini JC, Romero P. Photoaffinity Labeling of the T Cell Receptor on Cloned Cytotoxic T Lymphocytes by Covalent Photoreactive Ligand. J. Biol. Chem 1994;269:5574–5582. [PubMed: 8119892]
45. Love PE, Shores EW. ITAM multiplicity and thymocyte selection: how low can you go? Immunity 2000;12:591–597. [PubMed: 10894159]
46. Yachi PP, Ampudia J, Zal T, Gascoigne NRJ. Altered peptide ligands induce delayed CD8-T cell receptor interaction - a role for CD8 in distinguishing antigen quality. Immunity 2006;25:1046–1054.
47. Goldrath AW, Hogquist KA, Bevan MJ. CD8 lineage commitment in the absence of CD8. Immunity 1997;6:633–642. [PubMed: 9175841]

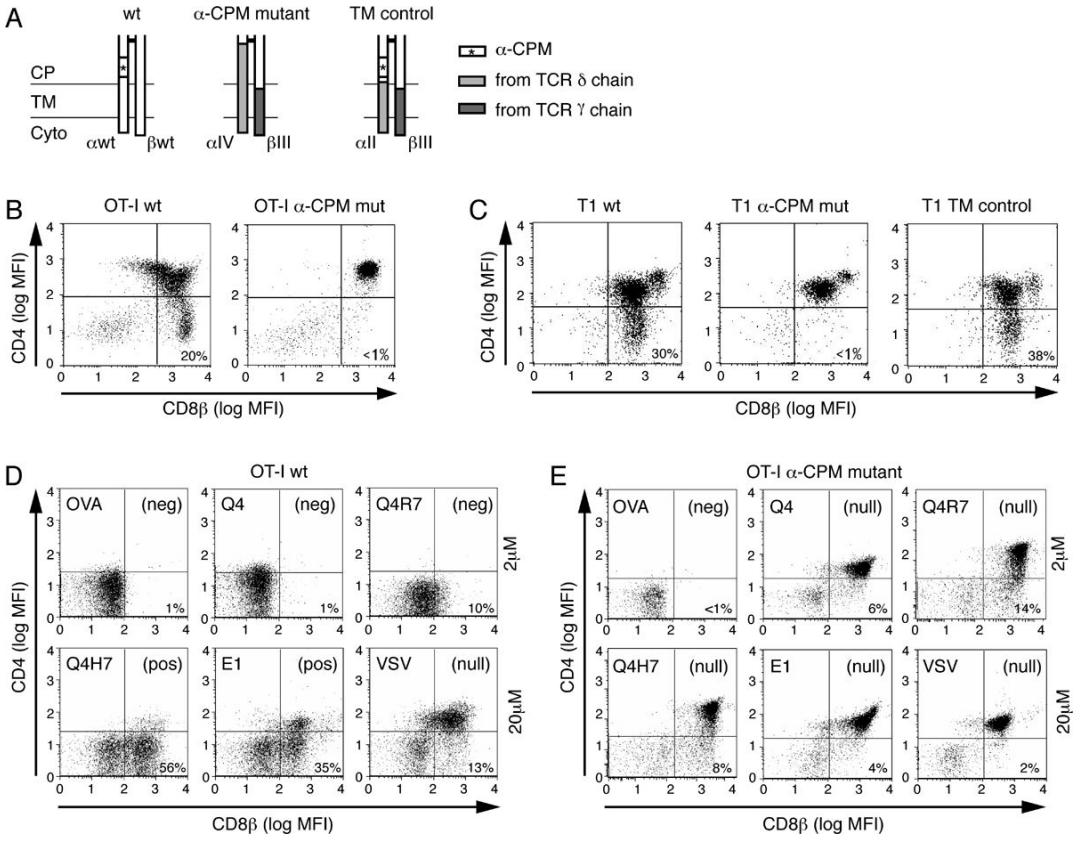

Fig. 1. Schematic representation of the TCR constant regions used in this study and characterization of the peptide variants

A, Schematic representation of the connecting peptide (CP), transmembrane (TM) and cytoplasmic (Cyt) domains of the wildtype and chimeric TCRs used. The α-CPM sequence is indicated with an asterisk (*). Open bars, TCRα and TCRβ sequences; light grey bars, TCRδ sequences; dark grey bars, TCRγ sequences. The α-CPM mutant receptor (αIV/βIII) is similar to the TM control receptor (αII/βIII), except that the α-CPM has been removed and replaced by the corresponding TCRδ sequence in the αIV chain (26).

B, Flow cytometric analysis of thymocytes expressing wildtype or α-CPM mutant OT-I TCR (as previously shown (28)). Thymocytes from C57Bl/6 Rag2−/− mice, transgenic for the wildtype or α-CPM mutant TCR, were stained with monoclonal antibodies against CD4 and CD8β. The numbers in the dot plots indicate the percentage of CD8αβ+ CD4−single positive cells.

C, Flow cytometric analysis of thymocytes expressing wildtype, α-CPM mutant or TM control T1 TCR. Thymocytes from BALB/c Rag2−/− mice, which were transgenic for the wildtype, α-CPM mutant or TM control TCR, were stained and analyzed as in B. D and E, Fetal Thymic Organ Culture (FTOC) analysis. Thymi from day 15.5 embryos of either OT-I wildtype (D) or α-CPM mutant (E) Rag−/− β2m−/− mice were incubated with exogenously added individual peptide and β2m. The ability of a peptide to induce the differentiation of CD8αβ+ CD4−single positive cells was analyzed by flow cytometry after 7 days of culture. Cells were electronically gated for TCRβ expression and the CD4/CD8β expression profiles are shown with the percentage of CD8αβ+ CD4− SP cells indicated. In wild type FTOCs, the pattern of negative selection (neg) seen with 2 μM peptide is also seen over a broad concentration range of negative selecting peptides (data not shown). Positive selection (pos) in FTOC is more efficient using higher peptide concentrations; FTOCs stimulated with 20 μM peptide are shown in the figure. Lack of positive or negative selection is indicated by (null).

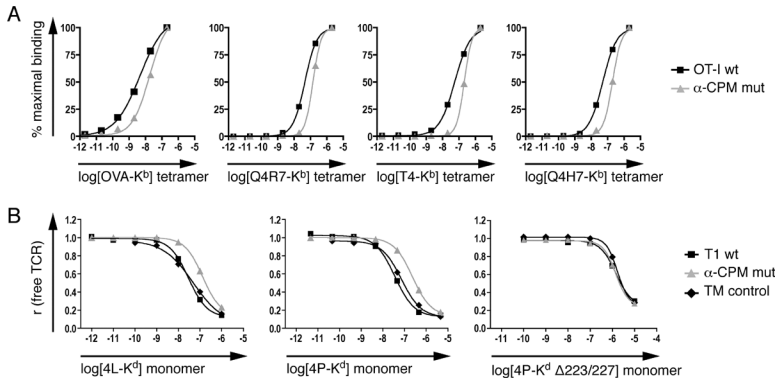

Fig. 2. Ligand binding of thymocytes with wildtype or mutant α-CPM TCRs

A, pMHC tetramer binding to thymocytes expressing OT-I wildtype or α-CPM mutant TCRs. Thymocytes from C57Bl/6 Rag−/− β2m−/− mice expressing either the wildtype or α-CPM mutant OT-I TCR were incubated with various PE-labeled tetramers at indicated concentrations at 37°C. Binding was quantified by flow cytometry and non-linear regression analysis. A representative experiment of at least 3 independent experiments is shown.

B, pMHC monomer binding to thymocytes expressing the T1 wildtype, α-CPM mutant or TM control TCR. Thymocytes from BALB/c Rag−/− β2m−/− mice expressing the T1 TCR variants were subjected to two-step labeling experiments as described (21). pMHC Δ223/227 monomers that significantly reduce CD8 binding were used with the 4P ligand (right panel). A representative experiment from a total of two or more independent experiments is shown.

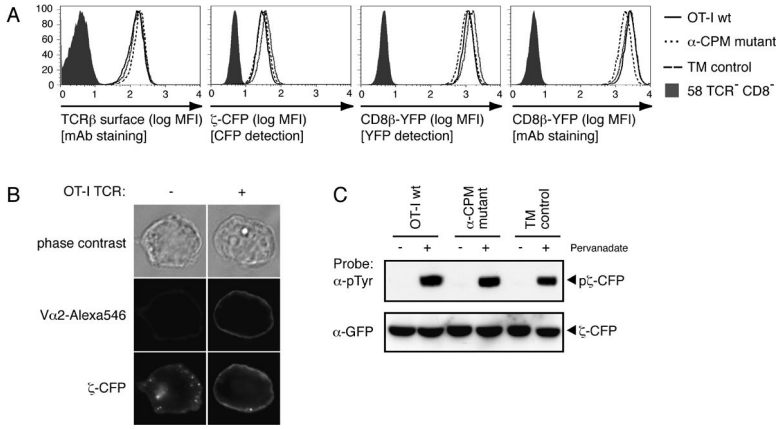

Fig. 3. Characterization of T-cell hybridomas

A, OT-I TCR, CD3ζ-CFP and CD8β-YFP expressed on wildtype, α-CPM mutant and TM control T-cell hybridomas were analyzed by flow cytometry. CD3ζ-CFP expression was measured by CFP detection. CD8β-YFP expression was measured by a fluorescent monoclonal antibody to CD8β and YFP detection.

B, Expression and localization of CD3ζ-CFP. When OT-I wt TCR is expressed on the cell surface, CD3ζ-CFP localizes to the plasma membrane. TCR expression is shown upon staining with anti-Vα2 and Alexa546.

C, Phosphorylation of the CD3ζ-CFP construct. 20×10^6 OT-I wt or α-CPM mutant hybridomas were treated with 100μM pervanadate. Cell lysates were immunoprecipitated with rabbit anti-GFP (Epitomics) and then probed with anti-phosphotyrosine (4G10) monoclonal antibody. Stripping and reprobing with mouse anti-GFP (Santa Cruz) revealed the presence of CD3ζ-CFP in all samples.

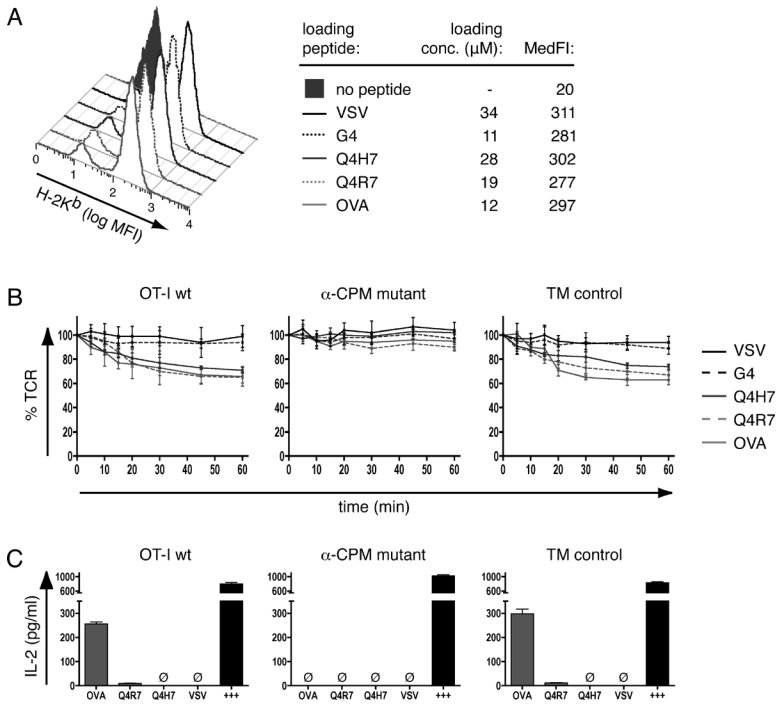

Fig. 4. Stimulation of T-cell hybridomas with peptide-loaded APCs

A, Peptide-loading of RMA-S cells. RMA-S cells were loaded with indicated concentrations of peptide as described in materials and methods. Staining with a fluorescently labeled H2-K^b antibody and flow cytometric analysis revealed similar median fluorescence intensities (MedFI) and therefore similar peptide-K^b expression with all peptides.

B, TCR internalization. T-cell hybridomas were stimulated with peptide-loaded RMA-S cells (loading concentration as indicated in A). At indicated time points, TCR expression was determined by flow cytometry. TCR expression was set as 100% at 0 min and MFI signals were normalized to those values.

C, IL-2 production. T-cell hybridomas were stimulated with peptide-loaded RMA-S cells (loading concentration as indicated in A). After 24h, supernatants were harvested and the amounts of IL-2 determined by ELISA. Calcium ionophore/PHA/PMA stimulation was used as positive control (+++). Ø = not detected

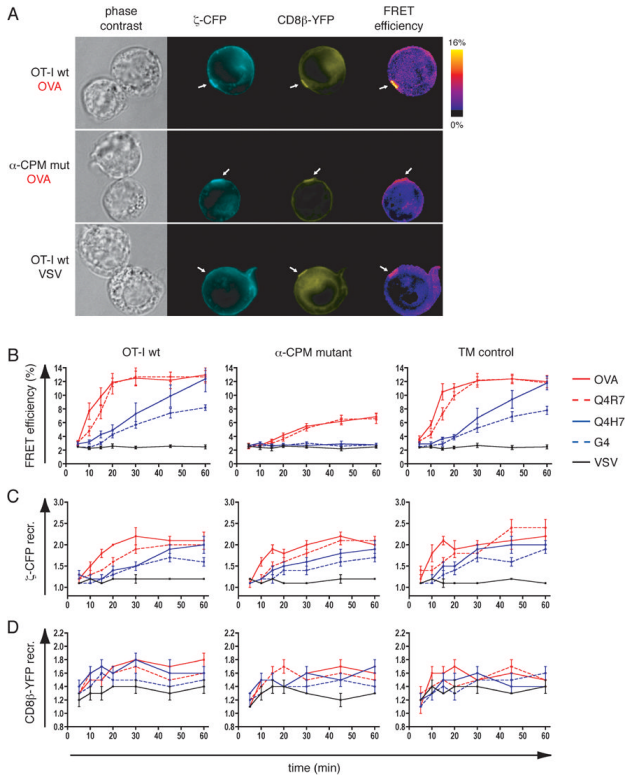

Fig. 5. Ligand induced CD3ζ-CD8β interaction

A, Fluorescence images of conjugates between peptide loaded APCs and OT-I wt or α-CPM mutant hybridomas (loading concentration as indicated in Fig. 4A). Conjugates are shown as phase contrast images, CD3ζ-CFP in cyan, CD8β-YFP in yellow and FRET efficiency images as donor-ratioed, compensated color gradients according to the algorithm described in materials and methods. The color code is depicted in the scale bar. White arrows indicate synapses.

B, CD3ζ-CFP and CD8β-YFP FRET measurements at the interface of T-cell hybridomas:APC conjugates. The indicated average values ± s.e.m. originate from n≥20 conjugates for OVA, Q4R7, Q4H7, G4 and n≥10 for VSV. Negative-selecting ligands (OVA, Q4R7) are depicted in red and positive-selecting ligands (Q4H7, G4) in blue. The non-cognate VSV ligand is shown in black. For OT-I wt and TM control hybridomas, the differences in FRET efficiency induced by the weakest negative selector Q4R7 or the strongest positive selector Q4H7 were significant ($p < 0.05$) at 10min, 15min, 20min and 30min. For the α-CPM mutant hybridomas, the differences in FRET signals induced by Q4R7 or Q4H7 were significant ($p < 0.05$) at 20min, 30min, 45min and 60min. To compare the same ligands between the T-cell hybridomas, we compared FRET signals between the α-CPM mutant and the TM control hybridoma. For Q4R7, the FRET signals were significantly different for all time points ($p < 0.05$). For Q4H7, the FRET signals in these two cell lines differed at 10min, 15min, 20min, 30min, 45min and 60min.

C, D, Recruitment of CD3ζ-CFP (C) and CD8β-YFP (D) to the synapse. Fold recruitment of CD3ζ-CFP and CD8β-YFP to the synapse were calculated as described in materials and methods. The values are indicated as mean ± s.e.m. and originate form n≥20 conjugates for OVA, Q4R7, Q4H7, G4 and n≥10 conjugates for VSV.

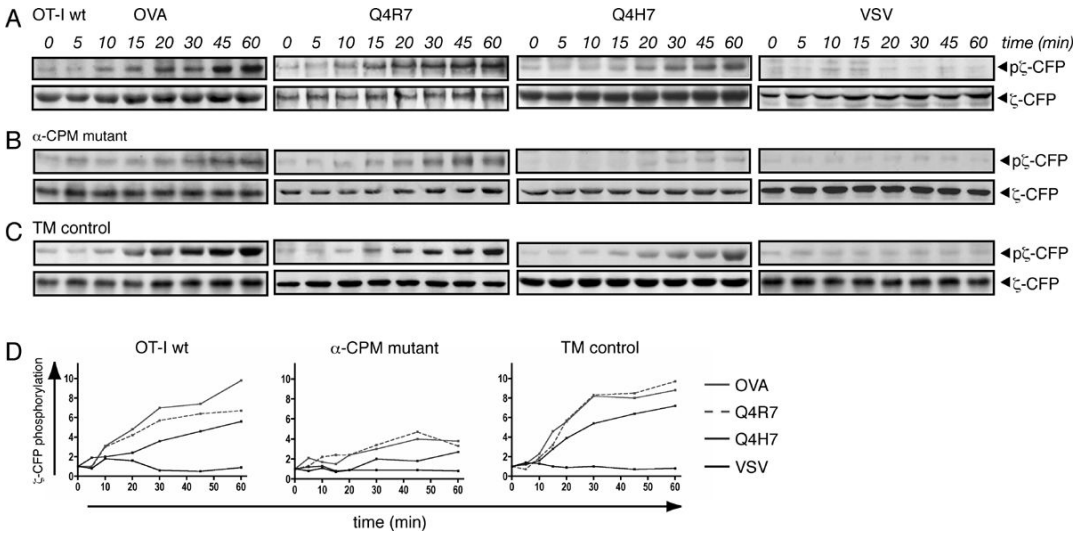

Fig. 6. Ligand induced CD3ζ-CFP phosphorylation

A, Tyrosine phosphorylation of CD3ζ-CFP. OT-I wt hybridomas were stimulated with peptide-loaded APCs. CD3ζ-CFP phosphorylation was assessed by immunoprecipitation and western blotting. Anti-phosphotyrosine monoclonal antibody (4G10) indicates phosphorylated CD3ζ-CFP. Only one species of phosphorylated CD3ζ-CFP could be observed (~50 kDa) in contrast to endogenous CD3ζ, which exhibits phosphorylated forms of increased molecular sizes (45). For signal normalization, membranes were stripped and probed with anti-GFP monoclonal antibody. Representative blots are shown (n≥2).

B, α-CPM mutant and C, TM control T-cell hybridomas were probed for CD3ζ-CFP phosphorylation as described in A.

D, Densitometric evaluation of CD3ζ-CFP phosphorylation. Densitometry of the western blots from panels A to C was performed using a phosphoimager (ChemiImager 5500, Alpha Innotech). Mean intensity values were normalized to the values obtained at 0 min and to the anti-GFP signal using the Alpha Ease Fc (Alpha Innotech) software.

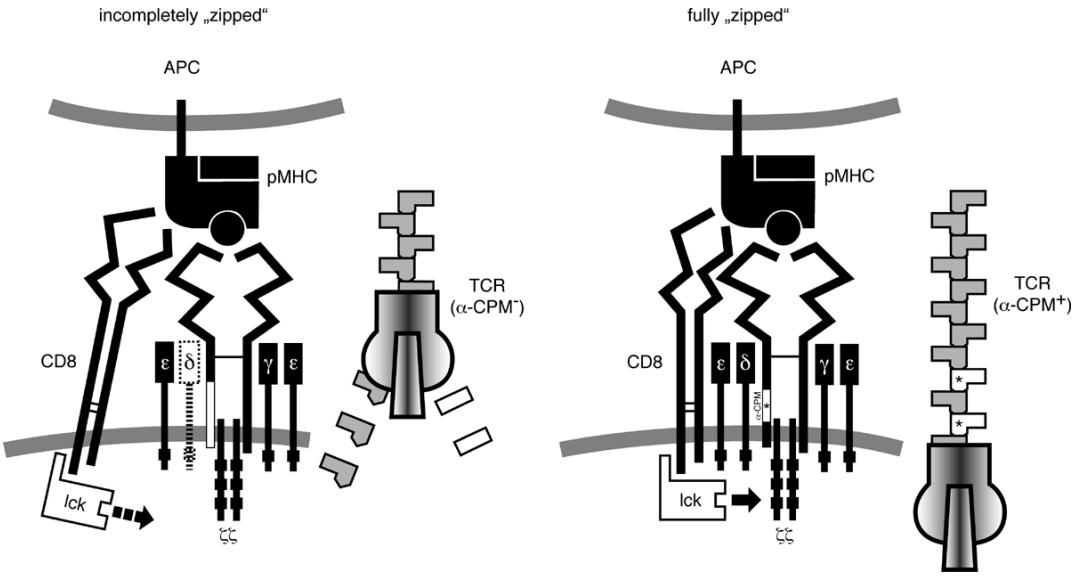

Fig. 7. The zipper model of TCR-CD8 approximation

In absence of an intact α-CPM, the CD8 co-receptor binds to the pMHC but only inefficiently engages the TCR at the level of the transmembrane and cytoplasmic domains. A candidate for linking the TCR and the CD8 co-receptor is the CD3δ molecule, which has been previously shown to be poorly associated to the TCR/CD3 complex in α-CPM deficient cells (26) (29), which is indicated in the left panel. In analogy to a zipper, the α-CPM receptor is missing a tooth, which hinders further zippering in the direction of the T-cell plasma membrane (left image). As a consequence, the ITAMs of the CD3 complex, especially CD3ζ, are inadequately phosphorylated. Only high-affinity ligands with a sufficiently long half-life of TCR binding can compensate for the α-CPM mutation. An intact α-CPM therefore allows tight CD8 association and closure of the zipper. In our model, this corresponds to a fully “zipped” approximation (right panel) where the co-receptor associated Lck can fully access the ITAMs of the CD3 complex.

Table I

K_D values for pMHC tetramer and monomer binding

A, K_D values [M] determined for pMHC tetramer binding to OT-I wildtype or α-CPM mutant $CD4^+CD8^+$ DP thymocytes. ΔK_D represents K_D α-CPM mutant / K_D wildtype. B, K_D values determined for pMHc monomer binding to T1 wildtype, α-CPM mutant or TM control $CD4^+CD8^+$ DP thymocytes Mean values of three experiments are shown. ΔK_D represents K_D α-CPM mutant / K_D TM control.

A

	Tetramer ligand			
Strain:	**OVA-K^b**	**Q4R7-K^b**	**T4-K^b**	**Q4H7-K^b**
OT-I wt	4.4×10^{-9}	4.5×10^{-8}	5.5×10^{-8}	5.0×10^{-8}
α-CPM cut	1.7×10^{-8}	1.4×10^{-7}	2.1×10^{-7}	2.0×10^{-7}
ΔK_D ($K_{D\ \alpha\text{-CPM}}$ / $K_{D\ wt}$)	**3.9 x**	**3.1 x**	**3.8 x**	**4.0 x**

B

	Monomer ligand		
Strain:	**4L-K^d**	**4P-K^d**	**4P-K^d Δ223/227**
T1 wt	2.8×10^{-8}	8.8×10^{-8}	1.4×10^{-6}
α-CPM mut	1.5×10^{-7}	3.9×10^{-7}	1.4×10^{-6}
TM control	3.5×10^{-8}	9.5×10^{-8}	1.7×10^{-6}
ΔK_D ($K_{D\ \alpha\text{-CPM}}$ / $K_{D\ TM\ ctrl.}$)	**4.3 x**	**4.1 x**	**0.8 x**